Cytotherapy, 2012; 14: 1011–1021

informa
healthcare

Transplantation of bone marrow cells decreases tumor necrosis factor-α production and blood–brain barrier permeability and improves survival in a mouse model of acetaminophen-induced acute liver disease

BRUNO SOLANO DE FREITAS SOUZA[1,2], RAMON CAMPOS NASCIMENTO[3,4], SHEILLA ANDRADE DE OLIVEIRA[1,5], JULIANA FRAGA VASCONCELOS[1,2], CARLA MARTINS KANETO[2], LIAN FELIPE PAIVA PONTES DE CARVALHO[2], RICARDO RIBEIRO-DOS-SANTOS[1,2], MILENA BOTELHO PEREIRA SOARES[1,2] & LUIZ ANTONIO RODRIGUES DE FREITAS[3,4]

[1]*Laboratório de Engenharia Tecidual e Imunofarmacologia, Centro de Pesquisas Gonçalo Moniz, Fundação Oswaldo Cruz, Salvador, BA, Brazil,* [2]*Centro de Biotecnologia e Terapia Celular, Hospital São Rafael, Salvador, BA, Brazil,* [3]*Laboratório de Patologia e Biointervenção, Centro de Pesquisas Gonçalo Moniz, Fundação Oswaldo Cruz, Salvador, BA, Brazil,* [4]*Faculdade de Medicina, Universidade Federal da Bahia, Salvador, BA, Brazil, and* [5]*Laboratório de Imunopatologia e Biologia Molecular, Centro de Pesquisas Aggeu Magalhães, Fundação Oswaldo Cruz, Recife, PE, Brazil*

Abstract

Background aims. Acute liver failure (ALF), although rare, remains a rapidly progressive and frequently fatal condition. Acetaminophen (APAP) poisoning induces a massive hepatic necrosis and often leads to death as a result of cerebral edema. Cell-based therapies are currently being investigated for liver injuries. We evaluated the therapeutic potential of transplantation of bone marrow mononuclear cells (BMC) in a mouse model of acute liver injury. *Methods.* ALF was induced in C57Bl/6 mice submitted to an alcoholic diet followed by fasting and injection of APAP. Mice were transplanted with 10^7 BMC obtained from enhanced green fluorescent protein (GFP) transgenic mice. *Results.* BMC transplantation caused a significant reduction in APAP-induced mortality. However, no significant differences in serum aminotransferase concentrations, extension of liver necrosis, number of inflammatory cells and levels of cytokines in the liver were found when BMC- and saline-injected groups were compared. Moreover, recruitment of transplanted cells to the liver was very low and no donor-derived hepatocytes were observed. Mice submitted to BMC therapy had some protection against disruption of the blood–brain barrier, despite their hyperammonemia, and serum metalloproteinase (MMP)-9 activity similar to the saline-injected group. Tumor necrosis factor (TNF)-α concentrations were decreased in the serum of BMC-treated mice. This reduction was associated with an early increase in interleukin (IL)-10 mRNA expression in the spleen and bone marrow after BMC treatment. *Conclusions.* BMC transplantation protects mice submitted to high doses of APAP and is a potential candidate for ALF treatment, probably via an immunomodulatory effect on TNF-α production.

Key Words: *acetaminophen, acute liver failure, bone marrow mononuclear cells, brain edema, cell therapy, tumor necrosis factor*

Introduction

Acute liver failure (ALF) is caused by liver cell dysfunction, leading to coagulopathy, hepatic encephalopathy and death in previously healthy patients. The main cause of this illness is poisoning with acetaminophen (*N*-acetyl-paraaminophen; APAP) through unintentional overdoses or suicide attempts (1). This drug induces severe centrolobular hepatocellular necrosis and increases serum transaminase levels, in a dose-dependent manner. The extent of APAP-induced hepatic lesions is increased by fasting and alcohol consumption, both in animals and humans (2,3).

APAP is metabolized by cytochrome P450 to form *N*-acetyl-*p*-benzoquinone imine (NAPQI). This reactive metabolite depletes glutathione and covalently binds to cysteine groups on proteins, leading to inhibition of mitochondrial respiration, mitochondrial permeability transition, hepatic necrosis and inflammatory response (4,5). The consequent massive death of hepatocytes is followed by disturbances in the hepatic cycle of urea and an increase in serum

Correspondence: **Luiz A. R. de Freitas**, Centro de Pesquisas Gonçalo Moniz, Fundação Oswaldo Cruz, Rua Waldemar Falcão, 121, Candeal, Salvador, BA, CEP 40296–710, Brazil. E-mail: lfreitas@bahia.fiocruz.br.

(Received 15 February 2012; accepted 1 April 2012)

ISSN 1465-3249 print/ISSN 1477-2566 online
DOI: 10.3109/14653249.2012.684445

ammonia levels. In the brain, the ammonia excess is incorporated as glutamate by astrocytes to form glutamine, an organic osmolyte, which leads to oxidative/nitrosative stress, blood–brain barrier (BBB) disruption and increased cerebral blood flow (6,7). All of these features induce encephalopathy and brain edema, the main cause of death in humans after an APAP overdose. Furthermore, the systemic production of the pro-inflammatory cytokine tumor necrosis factor (TNF)-α is increased in patients with acute liver failure, and a growing body of evidence indicates this cytokine to be a central mediator promoting the development of encephalopathy in this condition (8).

The definitive treatment for APAP-induced acute liver failure is liver transplantation, limited by the shortage of donors and surgical risks (9). Research for therapeutic approaches has focused on the prevention of liver damage with anti-oxidants, control of brain edema and hepatic support with bio-artificial livers or hepatocyte transplantation (10). Cell-based therapies have also been investigated as treatments for liver lesions. Transplantation of bone marrow mononuclear cells (BMC) has been shown to ameliorate dysfunction in different organs, such as the heart, brain and liver. BMC are easy to isolate and comprise different cell populations that can produce anti-inflammatory molecules related with hepatic protection in acute liver failure (11,12). In this study we evaluated the therapeutic potential of BMC transplantation in a model of APAP-induced hepatotoxicity potentiated by alcohol consumption.

Methods

Animals and acute liver failure induction

Animals were handled according to the Fundação Oswaldo Cruz (FIOCRUZ) guidelines for animal experimentation and the experimental protocols were approved by local animal ethics committees. Four to 6-week-old male C57Bl/6 mice weighing approximately 20 g were raised and maintained at the Gonçalo Moniz Research Center/Oswaldo Cruz Foundation (Salvador, Brazil) in rooms with controlled temperature (22 ± 2°C) and humidity (55 ± 10%) and continuous air renovation. Animals were maintained with 10% alcohol solution in water for 3 weeks. Before APAP administration, they were fasted for approximately 12 h with free access to pure water. Fresh suspensions of 16 mL/kg APAP (All Chemistry, São Paulo, Brazil) were prepared in warm saline (40°C) and given at 300 mg/kg intraperitoneally (corresponding to a lethal dose of 70%). Control mice received the same volume of saline solution.

Transplantation of BMC

Bone marrow cells were obtained from femurs and tibiae of 4–6-week-old enhanced green fluorescent protein (EGFP)-transgenic C57Bl/6 mice. The mononuclear cell fraction was purified by centrifugation in a Histopaque gradient at 1000 ***g*** for 25 min at 25°C (Histopaque 1119 and 1077, 1:1; Sigma-Aldrich, St Louis, MO, USA). The mononuclear cell fraction was collected and washed three times in Dulbecco's modified Eagle medium (Sigma-Aldrich). Cell suspensions were filtered over nylon wool and diluted in saline (5×10^7 cells/mL), and their viability was evaluated by trypan blue exclusion (Sigma-Aldrich). The cells were injected into the peripheral circulation 3 h after APAP injection (1×10^7 cells/mouse). In addition, BMC samples were analyzed by flow cytometry in a FACScalibur flow cytometer using conjugated antibodies (Becton Dickinson, San Diego, CA, USA), showing that 96.5 ± 1.3% expressed green fluorescent protein (GFP) and 96.3 ± 3.1% expressed CD45. Hematopoietic progenitor markers Sca-1, CD34 and CD117 were expressed by 0.11 ± 0.03%, 0.20 ± 0.05% and 0.17 ± 0.04% of the cells, respectively.

Tissue preparation and evaluation of liver injury

Mice from BMC- and saline-treated groups were anesthetized with ketamine (115 mg/kg) and xylazine (10–15 mg/kg) at different time-points after APAP injection. The animals were immediately perfused transcardially with 50 mL cold 0.9% saline, followed by 100 mL cold 4% paraformaldehyde (Merk, Darmstadt, Germany) in phosphate-buffered saline (PBS), pH 7.2. Livers were excised and left lobes were fixed in 10% formalin and paraffin-embedded. Four micrometer-thick paraffin-embedded sections were stained with hematoxylin-eosin (H&E). Analyses were performed on whole liver sections after slide scanning using an Aperio ScanScope system (Aperio Technologies, Vista, CA, USA). The images were analyzed using the Image Pro program (version 7.0; Media Cybernetics, San Diego, CA, USA). Hepatic injury was determined as a percentage of necrotic tissue, and a mean area of 24 676 428 μm^2/mouse was analyzed.

Quantification of EGFP cells in the liver by immunofluorescence

After transcardiac perfusion with paraformaldehyde, non-left hepatic lobes were additionally fixed in 4% paraformaldehyde at 4°C for 24 h. These samples were then incubated overnight in 30% sucrose solution in PBS at 4%, embedded in medium for congeal tissue and frozen at –70°C. Four-micrometer thick

sections were stained using a rabbit anti-human albumin (DAKO, Glostrup, Denmark) followed by anti-rabbit IgG conjugated with Alexa Fluor 568 (Invitrogen, Carlsbad, CA, USA), and mounted with VectaShield Hard Set medium with 4′,6-Diamidino-2-Phenylindole (DAPI) for nuclear staining (Vector, Burlingame, CA, USA). GFP^+ cells were quantified in five randomly selected areas per animal at a magnification of 200×.

Biochemical analyses

Blood was carefully collected in lithium heparinized tubes at different time-points immediately before killing, to avoid hemolysis. Plasma was obtained by centrifugation of blood for 10 min at 9000 ***g*** and stored at 4°C. Ammonia, Aspartate transaminase (AST) and ALT were evaluated within 2 h of plasma isolation using commercial kits (Vitros, New Jersey, USA, and Roche/Hitachi, Tokyo, Japan).

Quantification of inflammation

Quantification of infiltration of inflammatory cells was performed in 5-mm thick liver sections frozen in Optimal Cutting Temperature Compound (OCT). The analysis was performed in sections obtained from the left hepatic lobe. For microscopic analysis, an Olympus FluoView 1000 confocal laser scanning microscope (Olympus, Tokyo, Japan) was used for image acquisition. Sections were immunostained with primary antibody against mouse CD45, diluted 1:100 (Caltag, Buckingham, UK) overnight at 4°C. The next day sections were washed in PBS and incubated for 1 h at room temperature with the secondary antibody against rat IgG conjugated with Alexa Fluor 568. A total of five images per mouse was obtained in random fields. A magnification of 200× was used in order to cover an area of 1 mm^2. Numbers of $CD45^+$ cells were counted manually using Image-Pro Plus v.7.0 software (Media Cybernetics). In order to avoid overestimation because of counting partial cells that appeared within the section, only cells with intact morphology and a visible nucleus were counted.

Analysis of cytokine production

TNF-α, interleukin (IL)-6 and IL-10 levels were measured in total liver extracts and serum. Liver proteins were extracted from 100 mg tissue/mL PBS to which 0.4 M NaCl, 0.05% Tween-20 and protease inhibitors (0.1 mM phenylmethanesulfonyl fluoride; (PMSF), 0.1 mM benzethonium chloride, 10 mM Ethylenediamine tetraacetic acid (EDTA) and 20 Kallikrein Inhibitor Unit (KIU) aprotinin A/100 mL) were added. The samples were centrifuged for 10 min at 3000 ***g*** and the supernatant was frozen at –70°C for later quantification. Cytokine levels were estimated using commercially available immunoassay enzyme-linked immunosorbent assay (ELISA) kits for mouse TNF-α, IL-6 and IL-10 (BD, Franklin Lakes, NJ, USA), according to the manufacturer's instructions. Briefly, 96-well plates were blocked and incubated at room temperature for 1 h. Samples were added in duplicates and incubated overnight at 4°C. Biotinylated antibodies were added and plates were incubated for 2 h at room temperature. A half-hour incubation with streptavidin–horseradish peroxidase conjugate at a dilution of 1:200 was followed by detection using 3,3′,5,5′- tetramethylbenzidine (TMB) peroxidase substrate and reading at 450 nm.

Real-time polymerase chain reaction data

RNA was harvested and isolated with TRIzol reagent (Invitrogen) and the concentration was determined by photometric measurement. The RNA quality was analyzed in a 1.2% agarose gel. A high-capacity cDNA reverse transcription kit (Applied Biosystems, Carlsbad, CA, USA) was used to synthesize cDNA of 2 μg RNA following the manufacturer's recommendations.

Real-time reverse transcription (RT)-polymerase chain reaction (PCR) assays were performed to detect the expression levels of TNF-α (Mm 00443258_m1), IL-10 (Mm 00439616_m1), endothelin-1 (EDN-1; Mm 00438656_m1), adrenomedullin (ADM) (Mm00437438_g1) and GFP (assay by design) using hydrolysis probes from Applied Biosystems. Quantitative (q)RT-PCR amplification mixtures were made with Universal master mix (Applied Biosystems) and a 7500 real-time PCR system (Applied Biosystems). The cycling

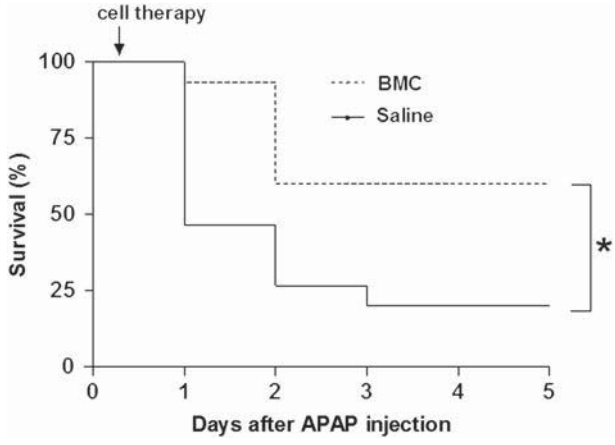

Figure 1. Effects of BMC therapy in APAP-induced lethality. Mice received saline or BMC 3 h after APAP injection. Survival was followed for 5 days. Results shown are from one experiment of four performed, each one with 15 mice/group. $^*P < 0.05$.

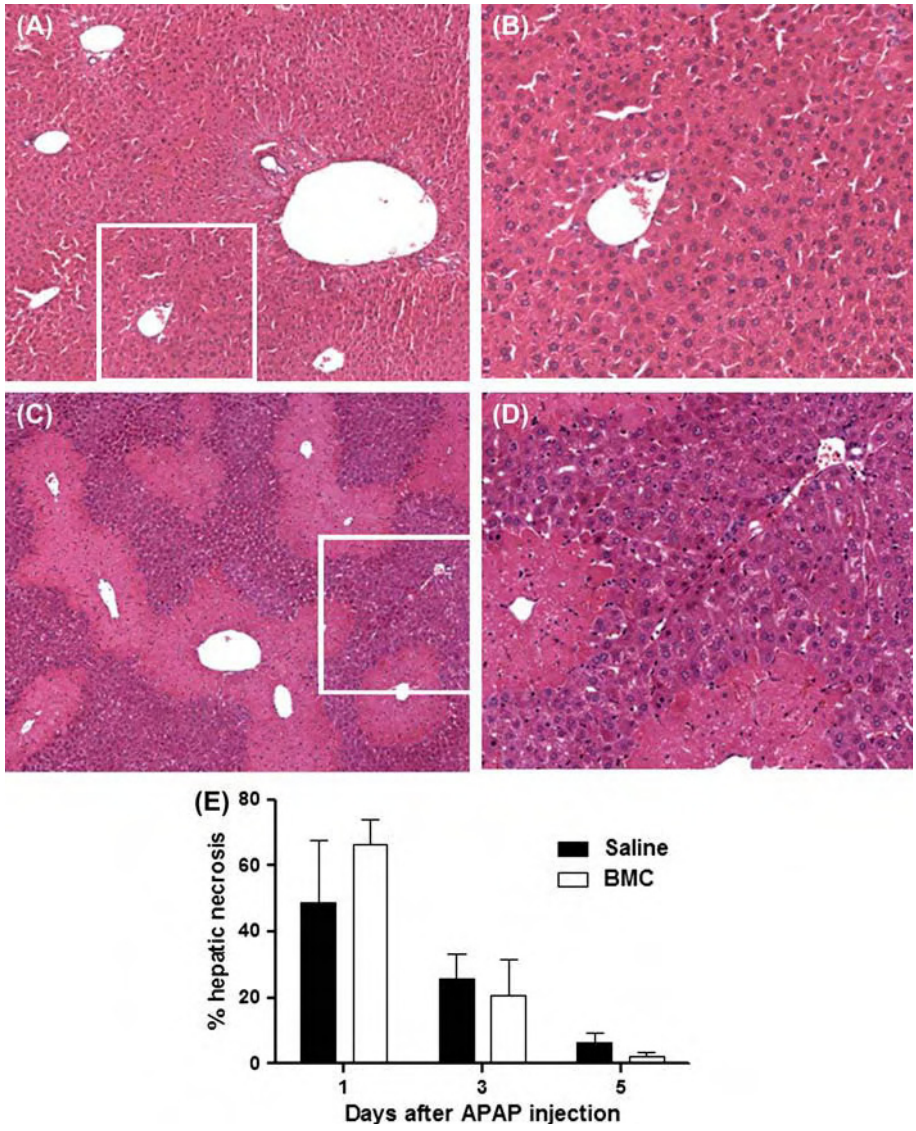

Figure 2. Liver necrosis after APAP injection and BMC transplantation. (A, B) Liver section of a mouse killed after 3 weeks of an alcoholic diet without APAP treatment, showing an absence of significant alteration of hepatic parenchyma. (C, D) Extensive centrolobular necrosis 24 h after APAP injection in the liver of saline-injected mice. (E) Quantification of the percentage of necrotic area in the liver parenchyma of saline-treated or BMC-treated mice. Results shown are from one of three experiments performed, each one with 3–5 mice/group/time-point.

conditions comprised 10 min polymerase activation at 95°C and 40 cycles at 95°C for 15 s and 60°C for 60 s. Normalization was made with the target internal control glyceraldehyde-3-phosphate dehydrogenase (GAPDH) using the cycle threshold method, and analysis of variance followed by the Tukey test.

Evaluation of BBB integrity

Evans blue (EB) has been used widely to assess brain edema (13). Mice were injected intravenously with 4 mL/kg 2% (w/v) EB solution. Thirty minutes later, the animals were killed with a ketamine overdose and brains were dissected away from the brainstem, cerebellum and meninges. Brain samples were embedded in medium for congeal tissue (Tissue-Tek) and frozen at –70°C. Five-micrometer thick sections were prepared, fixed in paraformaldehyde 4%, and nuclei stained with DAPI. EB+ cells were quantified in five randomly selected areas per animal at a magnification of 20×.

Metalloproteinase zymogram

Serum samples diluted 1:150 in non-reducing sample buffer (Tris–HCl buffer 500 mM/L, 10% glycerol, 4% Sodium Dodecyl Sulfate (SDS) w/v, 0.04% bromophenol blue w/v, pH 6.8) were loaded onto 7.5% SDS polyacrylamide gels containing type A gelatin from porcine skin 0.2% w/v (Sigma, St. Louis, MO, USA) and electrophoresis was performed at 100 V for

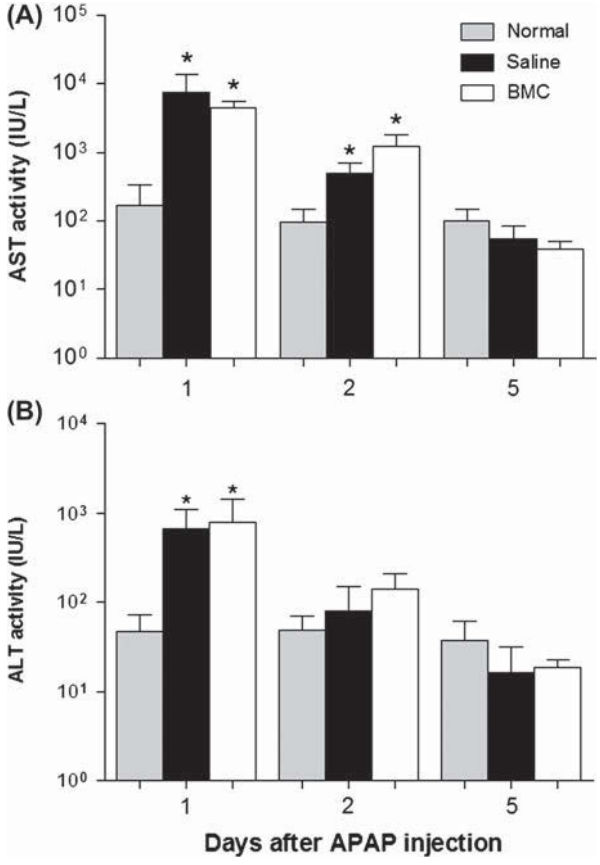

Figure 3. Measurement of serum levels of transaminases. (A) AST and (B) ALT serum levels of BMC- and saline-treated mice were determined at different time-points after APAP injection. Data obtained from one of two experiments performed represent the means ± SEM of 3–5 mice/group/time-point. $^{*}P < 0.05$.

3 h under cooling conditions (FB300 eletrophoresis power supply; Fisher Scientific, Waltham, MA, USA). Gels were then washed twice in 2.5% Triton X-100 solution for 30 min at room temperature with gentle agitation to remove SDS, and incubated at 37°C for 24 h in substrate buffer (Tris–HCl buffer 10 mM/L, 1.25% Triton X-100, $CaCl_2$ 5 mM/L, $ZnCl_2$ 1 μM/L, pH 7.5). Thereafter, gels were stained with a 0.5% w/v Coomassie blue R250 (Sigma-Aldrich) solution in 50% methanol, 10% acetic acid for 18 h and then unstained with the same solution without dye. Gelatinase activity was detected as unstained bands in a blue background, representing areas of proteolysis of the gelatin. After lamination and image acquisition, densitometric semi-quantitative analysis was performed using Scion image software (Image Program, National Institutes of Health, Scion Corporation, Frederick, MD, USA).

Statistical analyses

Results were expressed as mean ± SEM. Statistical comparisons were performed using Mann–Whitney or Kruskal–Wallis tests for non-parametric data. Parametric data were analyzed with *t*-test or ANOVA. Survival curves were evaluated by log-rank (Mantel–Cox) test, using Prism Software (version 5.0; GraphPad Software, San Diego, CA, USA). A *P*-value less than 0.05 was considered statistically significant.

Results

Transplantation of BMC reduces APAP-induced mortality without affecting hepatic necrosis

To evaluate the effect of BMC therapy in APAP-induced mortality, animals were injected with saline or BMC suspensions by an intravenous route 3 h after APAP injection. Five days later, the survival rate of the BMC-treated group was 60%, significantly higher than the 20% observed in the saline-injected group (Figure 1). On the other hand, when the same dose of BMC was given 9 h after APAP injection, this protective effect was not observed (data not shown).

Alcoholic diet alone did not result in any morphologic alterations visible by optic microscopy (Figure 2A, B). However, APAP administration after an alcoholic diet resulted in extensive necrosis in the centrolobular liver zone (Figure 2C, D). We did not observe any differences in necrosis extension (Figure 2E) and serum transaminase levels (Figure 3A, B) between BMC- and saline-treated groups at different time-points after APAP injection. To correct a possible selection bias in necrosis analysis as a result of mortality, an experiment was performed in which mice were organized in pairs containing one BMC- and one saline-treated mouse. Mortality was evaluated every 3 h after APAP injection. Livers from paired animals were immediately harvested after the death of any animal from each pair, and even then we did not observe differences in hepatic damage between BMC-treated and saline-injected mice (data not shown).

Transplanted BMC migrate to the liver but do not differentiate into hepatocytes or reduce local inflammation

Liver sections from BMC-treated mice were processed for analysis by immunofluorescence microscopy in order to track the presence of GFP^+ cells. Despite the inflammatory cell infiltrate in centrolobular areas observed in H&E sections, there was little recruitment of transplanted cells to hepatic parenchyma. The maximum engraftment occurred 24 h after APAP injection, when about 13 cells/mm^2 were found in liver sections (Figure 4B). Moreover, GFP^+ cells did not express albumin and did not show hepatocyte-like polygonal morphology at the time-points evaluated (Figure 4A). GFP^+ cell were also found in the spleens of BMC-transplanted mice (Figure 4C). The analysis of GFP mRNA expression in the bone marrow, spleens and livers of BMC-transplanted mice demonstrated that

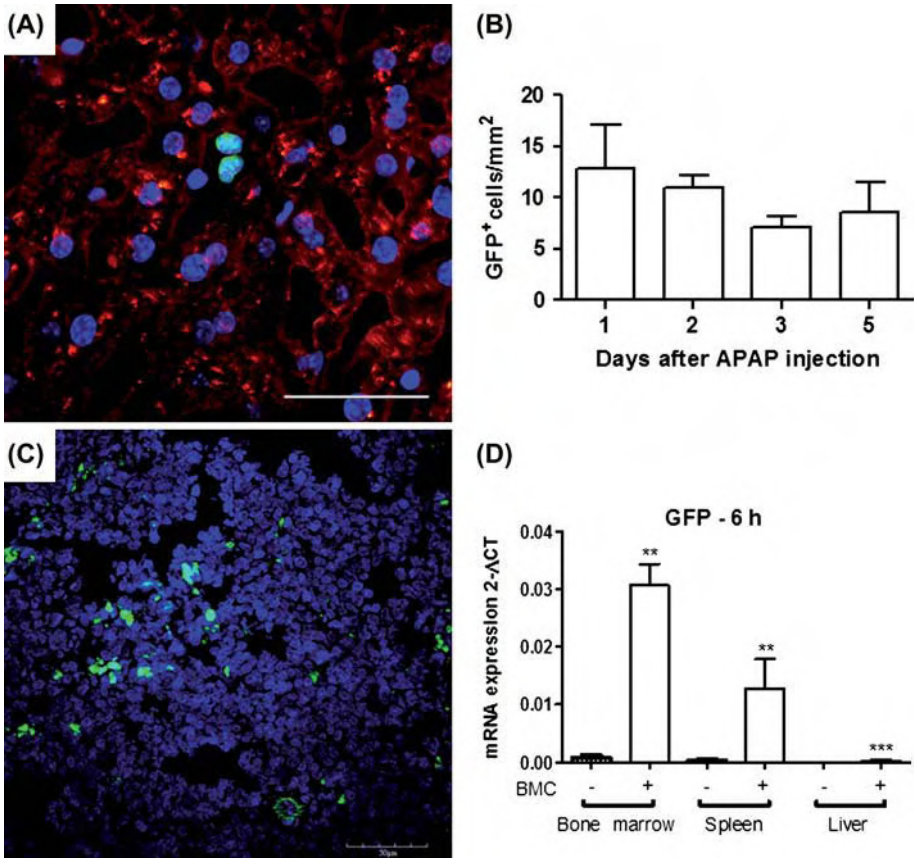

Figure 4. Migration of BMC to different organs with low recruitment to the injured liver. (A) Immunofluorescence of liver section showing a centrolobular zone from a BMC-treated mouse 5 days after APAP injection. Presence of GFP^+ cells (green) in sections stained with DAPI (blue) for nuclei visualization and with anti-albumin antibody (red). GFP^+ cells (green) on liver parenchyma did not express albumin and did not assume hepatocyte-like polygonal morphology. The section was counterstained with DAPI for nuclei visualization (blue). (B) Quantification of GFP^+ cells in livers of BMC-treated mice at different time-points after APAP injection. Data represent the means ± SEM of 3–5 mice/group/time-point. (C) The presence of GFP^+ cells (green) in the spleen section of a BMC-transplanted mouse. The section was counterstained with DAPI for nuclei visualization (blue). Bar = 50 μm. (D) GFP gene expression in bone marrow, spleen and liver of mice 6 h after APAP injection, showing increased recruitment of transplanted BMC to the bone marrow, followed by spleen and liver. Data represent mean ± SEM of seven mice/group. Scale bars represent 50 μm. $^*P < 0.05$; $^{**}P < 0.001$; $^{***}P < 0.0001$.

most of the cells migrated to the bone marrow and the spleen, and very few cells were retained in the liver 6 h after APAP injection (Figure 4D).

To evaluate the number of inflammatory cells, liver sections were submitted to immunofluorescence analysis using an antibody against the pan-leukocyte marker CD45. Mice injected with APAP had $CD45^+$ cell infiltrates of mild intensity after 6 h (Figure 5A), which increased after 14 h (Figure 5B). The percentage of $CD45^+$ cells did not differ significantly between BMC-treated and saline-injected groups (Figure 5C).

BMC transplantation protects the BBB integrity

We next evaluated leakage in the BBB by EB injection 18 h after APAP injection. The number of EB-stained neurons was significantly attenuated in brains of mice from the BMC-treated group in comparison with saline-injected mice (Figure 6A–C). However, we did not observe migration of GFP^+ cells to the brains of BMC-transplanted mice by fluorescence microscopy.

Because hyperammonemia is implicated in the pathogenesis of brain edema in acute liver damage (7), we determined the serum ammonia levels after APAP injection in cell- and saline-treated mice. Ammonia levels were similar in both groups (BMC, 680 ± 30.4 μg/dL; saline, 730 ± 57.7 μg/dL; $P = 0.4859$). These data indicated that the reduction in the brain vessel permeability associated with BMC transplantation was probably because of an ammonia-independent mechanism.

Another factor that may contribute to disruption of the BBB is the increased activity of metalloproteinases (MMP (14–16). We evaluated the activity of MMP-9 in the sera of mice submitted to APAP-induced injury. No significant differences in the activity of MMP-9 were found when BMC-treated and saline-injected mice were compared (Figure 6D). We

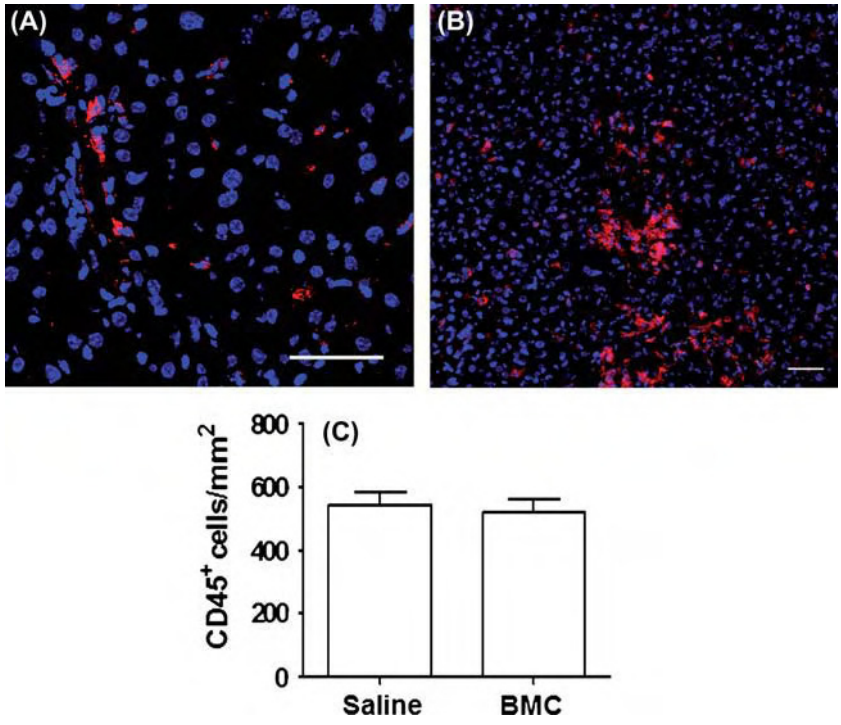

Figure 5. BMC transplantation does not affect the number of inflammatory cells in the liver. (A) Immunofluorescence showing mild infiltration of $CD45^+$ cells (red) into the injured liver 6 h after APAP injection. (B) Infiltration of $CD45^+$ cells into the liver increases 14 h after APAP injection. (C) Quantification of $CD45^+$ cells in the liver, showing similar numbers of infiltrating cells in both BMC- and saline-treated groups. Scale bars represent 50 μm. The data represent means ± SEM of seven mice/group.

then hypothesized that BMC could act by modulating the expression of adrenomedullin and endothelin-1, two peptides known for their role in the regulation of BBB permeability (17). Although the gene expression of adrenomedullin and endothelin-1 was found to be elevated in the brains of mice 14 h after APAP injection, no statistically significant difference was found between BMC- and saline-treated mice (Figure 6E, F).

Modulation of APAP-induced cytokine production after BMC transplantation

Because increased production of TNF-α is strongly associated with hepatic encephalopathy in acute liver failure (8), we measured the concentrations of TNF-α in the liver and serum of mice submitted to APAP-induced injury, as well as in normal controls. Saline-injected mice had increased TNF-α concentrations in the liver (Figure 7A) and serum (Figure 7C) when compared with normal controls. When BMC-treated mice were evaluated 14 h after APAP injection, we observed a significant reduction of TNF-α in the serum, but not in the liver, compared with saline-injected mice (Figure 7A, C).

To investigate the mechanisms by which BMC modulate TNF-α production, we measured the concentrations of the anti-inflammatory cytokine IL-10. IL-10 concentrations in the livers of BMC-transplanted and saline-injected mice were not significantly different (Figure 7B). However, when the expression of IL-10 mRNA was evaluated, a marked increase was observed in the spleen and bone marrow of BMC-transplanted mice 6 h after APAP injection (Figure 8A–D). Fourteen hours after APAP injection, gene expression of TNF-α was suppressed in the spleen, while IL-10 was up-regulated (Figure 8E, F).

Discussion

We have demonstrated a protective effect of BMC transplantation in mice with ALF induced by APAP. This was evidenced by a reduction in mortality, modulation of the production of inflammatory mediators and decreased damage to the BBB. This was only achieved when the cells were transplanted early (up to 6 h after APAP challenge), indicating that early events modulated by the cell therapy may be determinants of disease outcome.

The protective effect of BMC transplantation observed in our study did not correlate with an improvement in liver necrosis or function (ALT, AST and ammonia). However, in a rat model of ALF, improvement of liver function and decreased area of necrosis were observed after transplantation of BMC (18). This difference may be because of a slower evolution of the disease in the rat model

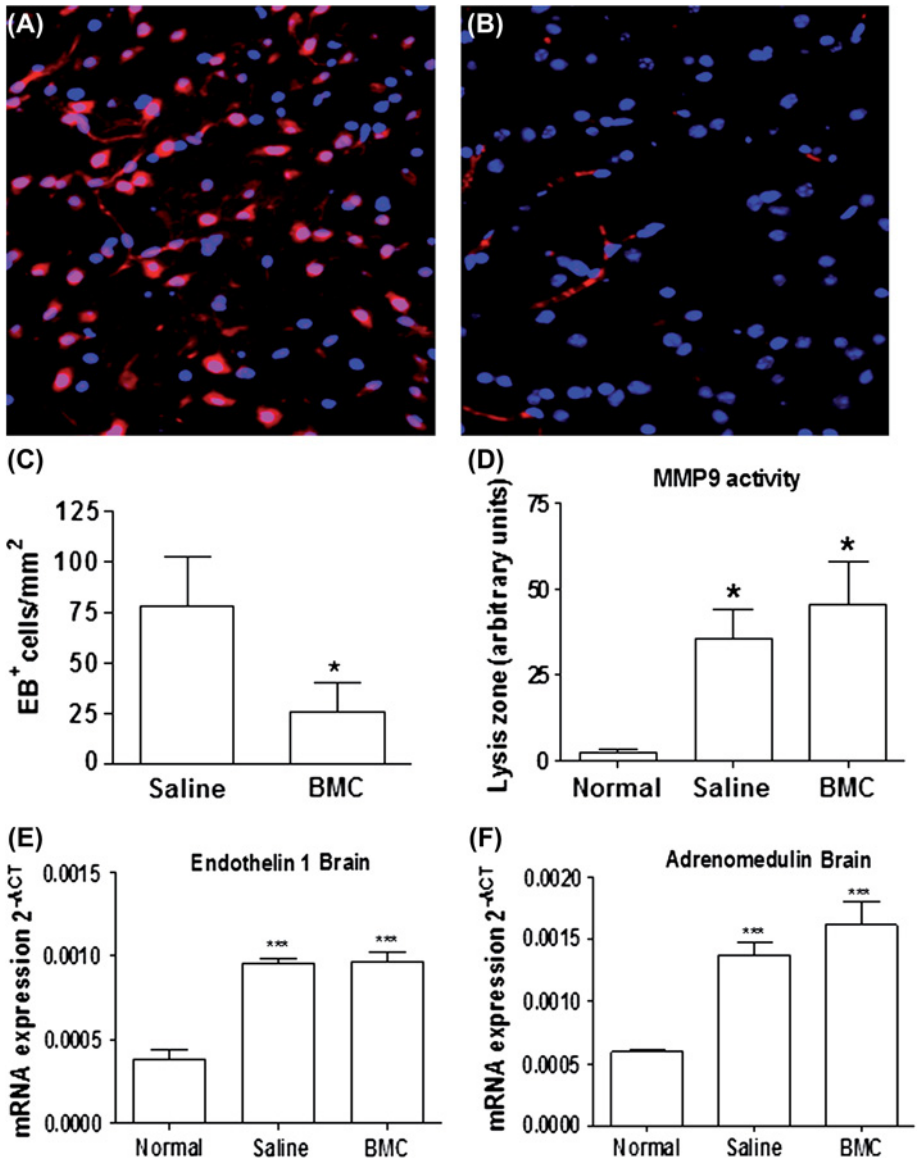

Figure 6. Evaluation of brain edema 18 h after APAP injection. Mice were injected with EB and killed 30 min later. Brains were processed as described in the Methods. (A, B) Fluorescence microscopy of brain sections obtained from saline- and BMC-treated mice, respectively. BMC induced low impregnation of cells with EB (red). Nuclei were stained with DAPI (blue). (C) EB staining cells were quantified in brain sections, and were reduced in BMC-treated mice. Data represent the means ± SEM of 3–5 mice/group. $^{*}P < 0.05$. (D) Zymogram for detection of serum MMP-9 activity 14 h after APAP injection, showing similar lysis area between BMC- and saline-treated groups. Data represent one of two experiments, presented as the means ± SEM of 12–14 mice/group. (E, F) qPCR analysis of gene expression of endothelin-1 (E) and adrenomedullin (F) in the brains of mice 14 h after APAP injection. Data represent the means ± SEM of 5–7 mice/group. $^{***}P < 0.0001$.

compared with the mouse model used in our study; most of the mice had died 24 h after APAP injection, whereas in the rat model mortality started after the first 24 h. Thus it is possible that, in our study, the fast evolution of the disease renders it difficult for the transplanted cells to promote any improvement of liver regeneration.

A few transplanted cells migrated to the liver, and no contribution of GFP^+ cells to hepatocyte formation was observed during all the time-points analyzed. Thus it is likely that the transplanted BMC act via a paracrine effect, causing the modulation of cytokine production in this model. In fact, a decrease in serum TNF-α concentrations and an increase in IL-10 mRNA expression in the bone marrow and spleen were observed after BMC transplantation in our model of ALF. The modulation of cytokine production and inflammatory response by BMC transplantation has been observed in other disease models, such as chronic chagasic cardiomyopathy (19), epilepsy (20) and chronic liver diseases (21).

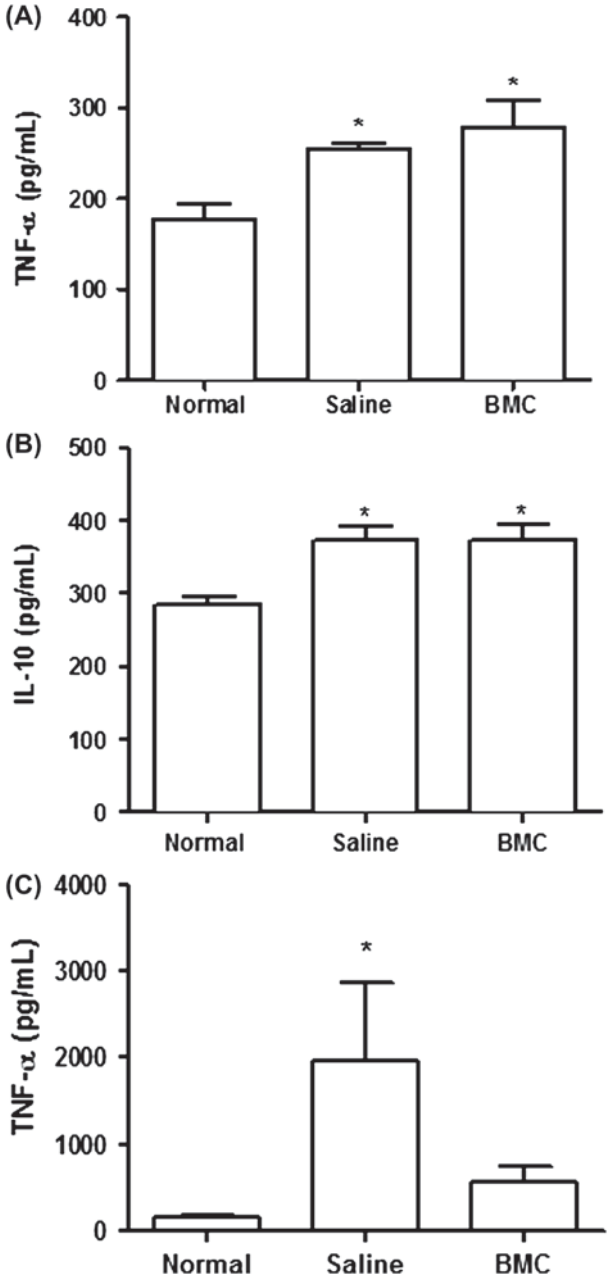

Figure 7. Assessment of cytokines in the liver and serum 14 h after APAP injection. Concentrations of TNF-α (A, C) and IL-10 (B) were determined in liver extracts (A, B) and serum (C) in saline- and BMC-treated mice 14 h after APAP injection. Data represent the means ± SEM of 5–7 mice/group. $^{***}P < 0.0001$.

The increase in TNF-α during the course of ALF seems to be a crucial event determining the disease outcome (22,23). TNF-α is a pleiotropic cytokine the effects of which may contribute in different ways to disease progression, including apoptosis induction, endothelial cell and platelet activation, increased vascular permeability and induction of soluble mediators (24). TNF-α elevation in ALF is indicated as one of the main causes of hepatic encephalopathy, and the severity of encephalopathy correlates with TNF-α serum concentration in patients with ALF (25). Elevated serum levels of TNF-α has been shown previously to correlate with increased permeability of the BBB in mice with APAP-induced ALF (26). Furthermore, Bemeur *et al.* (27), using an experimental model of ALF induced by azoxymethane in mice, have shown successfully that TNFR1 knockout mice are protected against the onset of coma and brain edema. Thus it is possible that the modulation of TNF-α production by transplanted BMC causes a decreased leakage in the BBB, consequently decreasing the development of hepatic encephalopathy and death rate of mice after APAP challenge.

TNF-α production was modulated in the serum but not in the liver of mice submitted to BMC transplantation after APAP challenge. This suggested a systemic immunomodulatory effect of the transplanted cells, and in fact an increase in IL-10 mRNA expression was observed both in the spleen as well as the bone marrow of BMC-treated mice 3 h after cell transplantation. The spleen and bone marrow are sites in which transplanted cells are preferentially retained (28), and this was confirmed in our study by qRT-PCR analysis. The production of IL-10, a potent anti-inflammatory cytokine with well-known suppressive activities over TNF-α production, has been described previously to occur in BMC cultures *in vitro* and *in vivo* in a model of myocardial infarct (29). Thus it is possible that both cell populations, transplanted cells as well as resident cells in the spleen and bone marrow, contribute to the increase in IL-10 mRNA expression.

In summary, we observed that peripheral transplantation of BMC reduced mortality in an APAP-induced model of acute liver failure potentialized by ethanol without improving liver damage. Transplanted cells did not differentiate into hepatocytes and did not up-regulate the liver function, as showed by serum ammonia dosage. Nonetheless, mice that received BMC transplantation showed less BBB injury. Studies are needed to evaluate the therapeutically active subpopulations in the BMC fraction and to describe the protective mechanisms involved.

Acknowledgments

The authors would like to acknowledge Dr Washington Luis Conrado dos Santos for his comments and discussions; Adriano Alcântara, Joselli Santos Silva, Elton Sá Barreto and Carine Machado Azevedo for technical assistance; CNPq, FINEP, MCT and FAPESB for financial support; LACEN, Salvador,

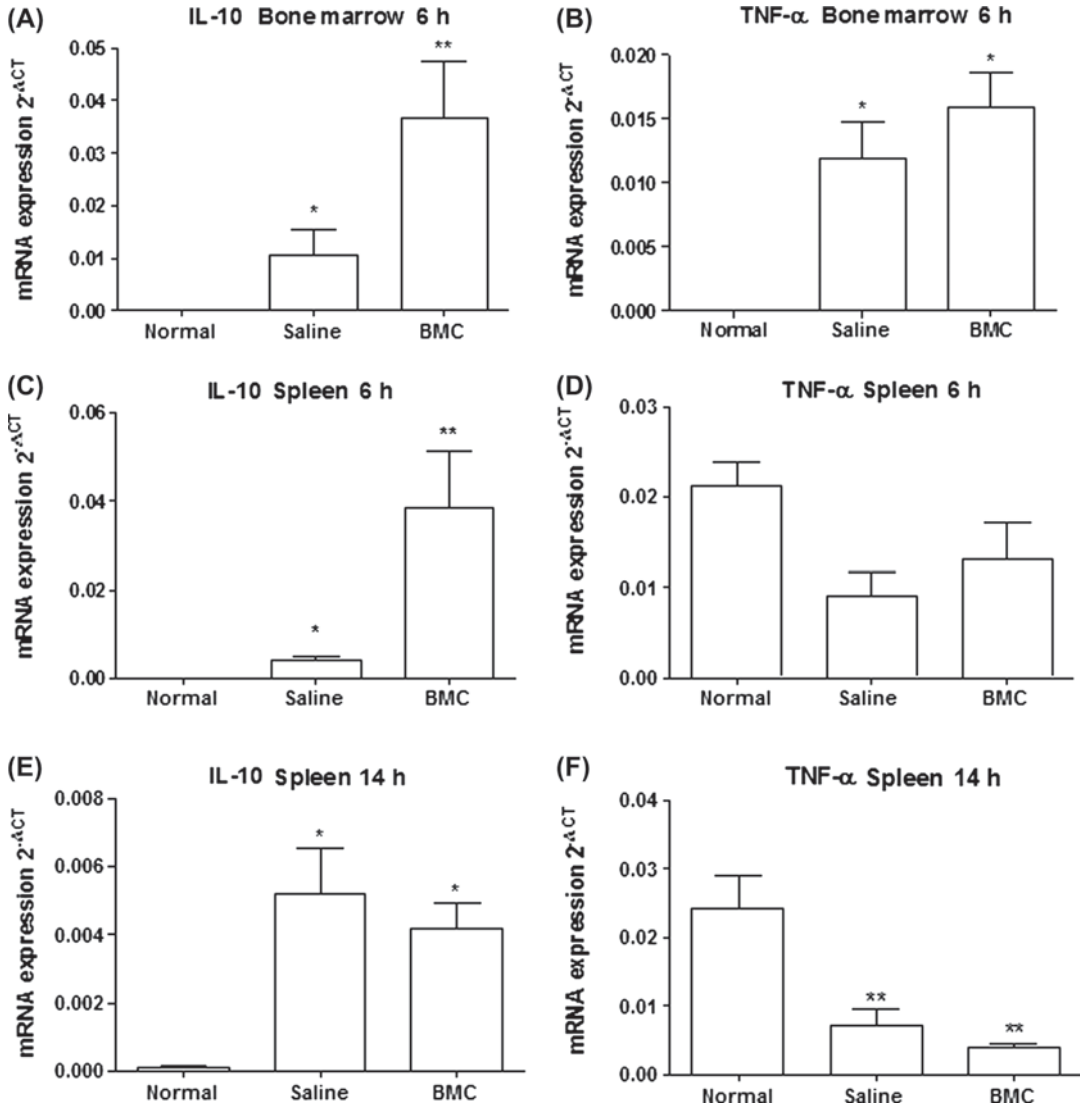

Figure 8. Measurement of cytokine gene expression in the bone marrow and spleen. (A, B) Analysis of IL-10 (A) and TNF-α (B) mRNA expression in the bone marrow 6 h after APAP injection. (C–F) Analysis of IL-10 (C, E) and TNF-α (D, F) mRNA expression in the spleen 6 (C, D) and 14 (D, F) h after APAP injection. Data represent the means ± SEM of 6–7 mice/group. $^{*}P < 0.05$; $^{**}P < 0.001$.

BA, for transaminase evaluation; and the Laboratory of Clinical Analysis of the Hospital São Rafael, Salvador, BA, for assessment of serum ammonia.

Conflict of interest statement: The authors claim they have no conflict of interest in this study.

References

1. Larson AM, Polson J, Fontana RJ, Davern TJ, Lalani E, Hynan LS, et al. Acetaminophen-induced acute liver failure: results of a United States multicenter, prospective study. Hepatology. 2005;42:1364–72.
2. Slattery JT, Nelson SD, Thummel KE. The complex interaction between ethanol and acetaminophen. Clin Pharmacol Ther. 1996;60:241–6.
3. Whitcomb DC, Block GD. Association of acetaminophen hepatotoxicity with fasting and ethanol use. J AM MED ASSOC. 1994;272:1845–50.
4. Potter WZ, Davis DC, Mitchell JR, Jollow DJ, Gillette JR, Brodie BB. Acetaminophen-induced hepatic necrosis. III. Cytochrome P-450-mediated covalent binding in vitro. J Pharmacol Exp Ther. 1973;187:203–10.
5. Masubuchi Y, Suda C, Horie T. Involvement of mitochondrial permeability transition in acetaminophen-induced liver injury in mice. J Hepatol. 2005;42:110–16.
6. Kosenko E, Kaminsky Y, Lopata O, Muravyov N, Kaminsky A, Hermenegildo C, et al. Nitroarginine, an inhibitor of nitric oxide synthase, prevents changes in superoxide radical and antioxidant enzymes induced by ammonia intoxication. Metab Brain Dis. 1998;13:29–41.
7. Chung C, Gottstein J, Blei AT. Indomethacin prevents the development of experimental ammonia-induced brain edema in rats after portacaval anastomosis. Hepatology. 2001;34: 249–54.
8. Odeh M. Pathogenesis of hepatic encephalopathy: the tumour necrosis factor-alpha theory. Eur J Clin Invest. 2007; 37:291–304.
9. Bernal W, Wendon J. Liver transplantation in adults with acute liver failure. J Hepatol. 2004;40:192–7.

10. Jalan R. Acute liver failure: current management and future prospects. J Hepatol. 2005;42(Suppl):S115–23.
11. Simpson K, Hogaboam CM, Kunkel SL, Harrison DJ, Bone-Larson C, Lukacs NW. Stem cell factor attenuates liver damage in a murine model of acetaminophen-induced hepatic injury. Lab Invest. 2003;83:199–206.
12. van Poll D, Parekkadan B, Cho CH, Berthiaume F, Nahmias Y, Tilles AW, et al. Mesenchymal stem cell-derived molecules directly modulate hepatocellular death and regeneration in vitro and in vivo. Hepatology. 2008;47:1634–43.
13. Abraham CS, Deli MA, Joo F, Megyeri P, Torpier G. Intracarotid tumor necrosis factor-alpha administration increases the blood–brain barrier permeability in cerebral cortex of the newborn pig: quantitative aspects of double-labelling studies and confocal laser scanning analysis. Neurosci Lett. 1996; 208:85–8.
14. Van Lint P, Wielockx B, Puimège L, Noël A, López-Otin C, Libert C. Resistance of collagenase-2 (matrix metalloproteinase-8)-deficient mice to TNF-induced lethal hepatitis. J Immunol. 2005;175:7642–9.
15. Wielockx B, Lannoy K, Shapiro SD, Itoh T, Itohara S, Vandekerckhove J, Libert C. Inhibition of matrix metalloproteinases blocks lethal hepatitis and apoptosis induced by tumor necrosis factor and allows safe antitumor therapy. Nat Med. 2001;7:1202–8.
16. Nguyen JH, Yamamoto S, Steers J, Sevlever D, Lin W, Shimojima N, et al. Matrix metalloproteinase-9 contributes to brain extravasation and edema in fulminant hepatic failure mice. J Hepatol. 2006;44:1105–14.
17. Kis B, Chen L, Ueta Y, Busija DW. Autocrine peptide mediators of cerebral endothelial cells and their role in the regulation of blood–brain barrier. Peptides. 2006;27: 211–22.
18. Belardinelli MC, Pereira F, Baldo G, Vicente Tavares AM, Kieling CO, da Silveira TR, et al. Adult derived mononuclear bone marrow cells improve survival in a model of acetaminopheninduced acute liver failure in rats. Toxicology. 2008;247:1–5.
19. Soares MB, Lima RS, Souza BS, Vasconcelos JF, Rocha LL, Dos Santos RR, et al. Reversion of gene expression alterations in hearts of mice with chronic chagasic cardiomyopathy after transplantation of bone marrow cells. Cell Cycle. 2011;10: 1448–55.
20. Costa-Ferro ZS, Souza BS, Leal MM, Kaneto CM, Azevedo CM, da Silva IC, et al. Transplantation of bone marrow mononuclear cells decreases seizure incidence, mitigates neuronal loss and modulates pro-inflammatory cytokine production in epileptic rats. Neurobiol Dis. 2012;46:302–13.
21. de Oliveira SA, de Freitas Souza BS, Barreto EP, Kaneto CM, Neto HA, Azevedo CM, et al. Reduction of galectin-3 expression and liver fibrosis after cell therapy in a mouse model of cirrhosis. Cytotherapy. 2012;14:339–49.
22. Streetz K, Leifeld L, Grundmann D, Ramakers J, Eckert K, Spengler U, et al. Tumor necrosis factor alpha in the pathogenesis of human and murine fulminant hepatic failure. Gastroenterology. 2000;119:446–60.
23. Nagaki M, Iwai H, Naiki T, Ohnishi H, Muto Y, Moriwaki H. High levels of serum interleukin-10 and tumor necrosis factor-alpha are associated with fatality in fulminant hepatitis. J Infect Dis. 2000;182:1103–8.
24. Idriss HT, Naismith JH. TNF alpha and the TNF receptor superfamily: structure-function relationship(s). Microsc Res Tech. 2000;50:184–95.
25. Odeh M. Pathogenesis of hepatic encephalopathy: the tumour necrosis factor-alpha theory. Eur J Clin Invest. 2007;37: 291–304.
26. Wang W, Lv S, Zhou Y, Fu J, Li C, Liu P. Tumor necrosis factor-α affects blood–brain barrier permeability in acetaminophen-induced acute liver failure. Eur J Gastroenterol Hepatol. 2011;23:552–8.
27. Bemeur C, Qu H, Desjardins P, Butterworth RF. IL-1 or TNF receptor gene deletion delays onset of encephalopathy and attenuates brain edema in experimental acute liver failure. Neurochem Int. 2010;56:213–15.
28. Aizawa S, Tavassoli T. Molecular basis of the recognition of intravenously transplanted hemopoietic cells by bone marrow. Proc Natl Acad Sci USA 1988;85:3180–3183.
29. Burchfield JS, Iwasaki M, Koyanagi M, Urbich C, Rosenthal N, Zeiher AM, Dimmeler S. Interleukin-10 from transplanted bone marrow mononuclear cells contributes to cardiac protection after myocardial infarction. Circ Res. 2008; 103:203–11.